

# Photoproduction of $\eta$ and $\eta'$ mesons off nucleons close to threshold<sup>1</sup>

B. Borasoy<sup>2</sup>

Physik Department  
Technische Universität München  
D-85747 Garching, Germany

## Abstract

The importance of Born terms and resonance exchange for  $\eta$  and  $\eta'$  photoproduction off both the proton and neutron within  $U(3)$  baryon chiral perturbation theory is investigated. Low-lying resonances such as the vector mesons and  $J^P = 1/2^+, 1/2^-$  baryon resonances are included explicitly and their contributions together with the Born terms are calculated. The coupling constants of the resonances are determined from strong and radiative decays. We obtain reasonable agreement with experimental data near threshold.

---

<sup>1</sup>Work supported in part by the DFG

<sup>2</sup>email: borasoy@physik.tu-muenchen.de

# 1 Introduction

Photoproduction of mesons is a tool to study baryon resonances and the investigation of transitions between these states provides a crucial test for hadron models. The dominance of the  $\Delta(1232)$  in the photoproduction of pions, e.g., has allowed to extract information on its electromagnetic transition amplitudes. Because of their hadronic decay modes nucleon resonances have large overlapping widths, which makes it difficult to study individual states, but selection rules in certain decay channels can reduce the number of possible resonances. The isoscalars  $\eta$  and  $\eta'$  are such examples since, due to isospin conservation, only the isospin- $\frac{1}{2}$  excited states decay into the  $\eta N$  and  $\eta' N$  channels. In recent years both  $\eta$  and  $\eta'$  photoproduction have been of considerable interest. The  $\eta$  photoproduction of protons has been measured at MAMI [1] and resonance parameters of the  $S_{11}(1535)$  resonance and the electromagnetic coupling  $\gamma p \rightarrow S_{11}$  have been extracted from the data. On the theoretical side, both an effective Lagrangian approach [2] and coupled channel models [3, 4] are used to investigate  $\eta$  photoproduction in the  $S_{11}(1535)$  resonance region. In these approaches the coupling of the  $\eta$  to the nucleons is described by both a pseudovector and a pseudoscalar term and the coupling constant and the coupling structure of the Born terms is unknown. In [4] it has been shown that differential cross sections are rather sensitive to the assumptions about this vertex. But within the framework of chiral perturbation theory this coupling is fixed at lowest order by making use of the chiral  $SU(3)_L \times SU(3)_R$  symmetry of the Lagrangian, whereas explicitly chiral symmetry breaking terms appear at higher orders. The  $SU(3)_L \times SU(3)_R$  symmetric limit provides therefore a convenient starting point which overcomes the problem of fixing the  $\eta NN$  vertex. The  $SU(3)$  chiral meson-baryon Lagrangian has been used in a coupled channel model [5] and by adjusting a few parameters a large amount of low-energy data was described. All the above mentioned investigations have in common that they treat the  $\eta$  meson as a pure  $SU(3)$  octet state  $\eta_8$  and mixing of  $\eta_8$  with the corresponding singlet state  $\eta_0$  which yields the physical states  $\eta$  and  $\eta'$  is neglected.

The  $\eta'$  is interesting by itself. The QCD Lagrangian with massless quarks exhibits an  $SU(3)_L \times SU(3)_R$  chiral symmetry which is broken down spontaneously to  $SU(3)_V$ , giving rise to a Goldstone boson octet of pseudoscalar mesons which become massless in the chiral limit of zero quark masses. On the other hand, the axial  $U(1)$  symmetry of the QCD Lagrangian is broken by the anomaly. The corresponding pseudoscalar singlet would otherwise have a mass comparable to the pion mass [6]. Such a particle is missing in the spectrum and the lightest candidate would be the  $\eta'$  with a mass of 958 MeV which is considerably heavier than the octet states. In conventional chiral perturbation theory the  $\eta'$  is not included explicitly, although it does show up in the form of a contribution to a coupling coefficient of the Lagrangian, a so-called low-energy constant (LEC).

The  $\eta'$  photoproduction has been investigated theoretically both in [7] and

[8]. In the effective Lagrangian approach of [7] a pseudoscalar coupling of the  $\eta'$  to the nucleons was chosen and it was concluded that the  $\eta'N$  decay channel is dominated by the not so well established  $D_{13}(2080)$  resonance, whereas in the quark model used in [8] the off-shell effects of the  $S_{11}(1535)$  were prominent. In contrast, the experimental data from ELSA [9] suggested the coherent excitation of two resonances  $S_{11}(1897)$  and  $P_{11}(1986)$ . Recently, the  $\eta'$  has been included in baryon chiral perturbation theory in a systematic fashion. Within this framework it is possible to calculate the importance of the  $S_{11}(1535)$  resonance for the  $\eta'N$  decay channel without making any assumptions on the  $\eta'NN$  coupling.

The aim of this paper is to clarify the role of Born terms and low-lying resonances for both  $\eta$  and  $\eta'$  photoproduction within the framework of baryon chiral perturbation theory. The simultaneous description of  $\eta$  and  $\eta'$  photoproduction will also allow the inclusion of the  $\eta$ - $\eta'$  mixing in a rigorous way. We restrict ourselves to the threshold region and to the calculation of Born terms and the leading resonances both in the  $t$ -channel and in the  $s$ - and  $u$ -channels. Such a simplified treatment of  $\eta$  and  $\eta'$  photoproduction will not allow us to reproduce all the experimental data in detail. Here, we are rather concerned with qualitative agreement and a rough estimate of the importance of low-lying resonances for both decay channels. In order to obtain a better description of the experimental data, one has to include chiral loops and further resonances, but this is beyond the scope of the present investigation. This work should therefore be considered to be mainly a check if the inclusion of  $\eta$  and  $\eta'$  mesons in a nonet of pseudoscalar mesons as proposed in [12] leads to an adequate description for processes of  $\eta$  and  $\eta'$  mesons with baryons.

The  $\eta$  photoproduction off the neutron which has been measured at ELSA [10] provides a further test of our simple model and we are able to give predictions for the cross sections for  $\eta'$  photoproduction off the neutron. In the next section, we present the necessary formalism for photoproduction of  $\eta$  and  $\eta'$  mesons. The effective chiral Lagrangian including explicitly low-lying resonances is given in Sec. 3. The invariant amplitudes are shown in Sec. 4 and Sec. 5 contains the numerical results. We conclude with a summary in Sec. 6. The determination of the baryon resonance couplings is relegated to the Appendix.

## 2 General Formalism

The  $T$ -matrix element for the processes  $N(p_1) + \gamma(k) \rightarrow N(p_2) + \phi(q)$  with  $\phi = \eta$  or  $\eta'$  is given by

$$\langle p_2, q \text{ out} | p_1, k \text{ in} \rangle = \delta_{fi} + (2\pi)^4 i \delta^{(4)}(p_2 + q - p_1 - k) T_{fi}. \quad (1)$$

The Mandelstam variables are

$$s = (k + p_1)^2 = (q + p_2)^2$$

$$\begin{aligned}
t &= (k - q)^2 = (p_1 - p_2)^2 \\
u &= (k - p_2)^2 = (q - p_1)^2
\end{aligned}
\tag{2}$$

subject to the constraint  $s + t + u = 2M_N^2 + m_\phi^2$  with  $M_N$  and  $m_\phi$  being the mass of the nucleon and the pseudoscalar meson, respectively. The invariant four-momentum transfer squared,  $t$ , can be related to the scattering angle  $\vartheta$  in the c.m. system via

$$t = m_\phi^2 - 2q^0 k^0 + 2|\mathbf{q}||\mathbf{k}|z \tag{3}$$

with  $z = \cos \vartheta$ . The equivalent photon energy in the laboratory system is given by

$$E_\gamma = \frac{s - M_N^2}{2M_N}, \tag{4}$$

and the threshold values of  $s, t$  and  $E_\gamma$  are

$$\begin{aligned}
s_{th} &= (M_N + m_\phi)^2 \\
t_{th} &= -\frac{m_\phi^2}{1 + \frac{m_\phi}{M_N}} \\
E_{\gamma,th} &= m_\phi \left(1 + \frac{m_\phi}{2M_N}\right).
\end{aligned}
\tag{5}$$

In the c.m. system, the differential cross section is related to  $T$  via

$$\begin{aligned}
\frac{d\sigma}{d\Omega_{cm}} &= \frac{1}{64\pi^2 s} \frac{\lambda^{1/2}(s, M_N^2, m_\phi^2)}{s - M_N^2} |T_{fi}|^2 \\
&= \frac{1}{64\pi^2 s} \frac{|\mathbf{q}|}{|\mathbf{k}|} |T_{fi}|^2
\end{aligned}
\tag{6}$$

with

$$\lambda(s, M_N^2, m_\phi^2) = [s - (M_N + m_\phi)^2][s - (M_N - m_\phi)^2], \tag{7}$$

and our normalization is such that  $\bar{u}u = 2M_N$ . In general,  $T$  can be decomposed as

$$T_{fi} = i\epsilon_\mu \bar{u}_2 \sum_{i=1}^8 B_i \mathcal{N}_i^\mu u_1 \tag{8}$$

with the invariant amplitudes

$$\begin{aligned}
\mathcal{N}_\mu^1 &= \gamma_5 \gamma_\mu \not{k}, & \mathcal{N}_\mu^2 &= 2\gamma_5 P_\mu, & \mathcal{N}_\mu^3 &= 2\gamma_5 q_\mu, \\
\mathcal{N}_\mu^5 &= \gamma_5 \gamma_\mu, & \mathcal{N}_\mu^6 &= \gamma_5 \not{k} P_\mu, & \mathcal{N}_\mu^8 &= \gamma_5 \not{k} q_\mu,
\end{aligned}
\tag{9}$$

where we have neglected the operators  $B_4$  and  $B_7$  since they vanish for real photons and we use  $P = \frac{1}{2}(p_1 + p_2)$ . From current conservation one obtains the relations

$$\begin{aligned}
B_3 &= -\frac{1}{2} \frac{s - u}{s + u - 2M_N^2} B_2 \\
B_5 &= -\frac{1}{4}(s - u)B_6 - \frac{1}{2}[s + u - 2M_N^2]B_8.
\end{aligned}
\tag{10}$$

It is therefore more convenient to define a set of independent amplitudes [11]

$$T_{fi} = i\bar{u}_2 \sum_{i=1}^4 A_i \mathcal{M}_i u_1 \quad (11)$$

with

$$\begin{aligned} \mathcal{M}_1 &= \frac{1}{2} \gamma_5 \gamma_\mu \gamma_\nu F^{\mu\nu}, & \mathcal{M}_2 &= 2\gamma_5 P_\mu q_\nu F^{\mu\nu}, \\ \mathcal{M}_3 &= \gamma_5 \gamma_\mu q_\nu F^{\mu\nu}, & \mathcal{M}_4 &= 2\gamma_5 \gamma_\mu P_\nu F^{\mu\nu} - 2M_N \mathcal{M}_1 \end{aligned} \quad (12)$$

and  $F_{\mu\nu} = \epsilon_\mu k_\nu - \epsilon_\nu k_\mu$ . The  $A_i$  obey the crossing relations

$$\begin{aligned} A_i(s, u) &= A_i(u, s) & i &= 1, 2, 4 \\ A_3(s, u) &= -A_3(u, s) \end{aligned} \quad (13)$$

and are related to the  $B_i$  via

$$\begin{aligned} A_1 &= B_1 - M_N B_6, & A_2 &= \frac{2}{s + u - 2M_N^2} B_2, \\ A_3 &= -B_8, & A_4 &= -\frac{1}{2} B_6. \end{aligned} \quad (14)$$

The differential cross section can be written in terms of products of the  $A_i$  with their complex conjugates  $A_i^*$

$$\frac{d\sigma}{d\Omega_{cm}} = \frac{1}{64\pi^2 s} \frac{\lambda^{1/2}(s, M_N^2, m_\phi^2)}{s - M_N^2} \sum_{i,j=1}^4 y_{ij} A_i A_j^*. \quad (15)$$

The coefficients  $y_{ij} = y_{ji}$  read

$$\begin{aligned} y_{11} &= [s - M_N^2][M_N^2 - u] \\ y_{12} &= \frac{1}{2} [t(su - M_N^4 + M_N^2 m_\phi^2) - M_N^2 m_\phi^4] \\ y_{13} &= \frac{M_N}{2} [s - u][m_\phi^2 - t] \\ y_{14} &= \frac{M_N}{2} [m_\phi^2 - t]^2 \\ y_{22} &= -t y_{12} \\ y_{23} &= y_{24} = 0 \\ y_{33} &= \frac{t}{4} [2M_N^4 - 2M_N^2 m_\phi^2 - s^2 - u^2] + \frac{1}{2} M_N^2 m_\phi^4 \\ y_{34} &= -\frac{t}{2M_N} y_{13} \\ y_{44} &= y_{33} - M_N^2 [m_\phi^2 - t]^2. \end{aligned} \quad (16)$$

The total cross section is obtained by integrating over the angular variable  $z = \cos \vartheta$

$$\sigma_{tot}(s) = 2\pi \int_{-1}^1 dz \frac{d\sigma}{d\Omega_{cm}}(s, z). \quad (17)$$

For the multipole decomposition one expresses the transition amplitude in terms of Pauli spinors and matrices

$$\frac{1}{8\pi\sqrt{s}} i\bar{u}_2 \sum_{i=1}^4 A_i \mathcal{M}_i u_1 = \chi_2^\dagger \mathcal{F} \chi_1. \quad (18)$$

The most general form for  $\mathcal{F}$  reads

$$\mathcal{F} = i\boldsymbol{\sigma} \cdot \boldsymbol{\epsilon} \mathcal{F}_1 + \boldsymbol{\sigma} \cdot \hat{\mathbf{q}} \boldsymbol{\sigma} \cdot (\hat{\mathbf{k}} \times \boldsymbol{\epsilon}) \mathcal{F}_2 + i\boldsymbol{\sigma} \cdot \hat{\mathbf{k}} \hat{\mathbf{q}} \cdot \boldsymbol{\epsilon} \mathcal{F}_3 + i\boldsymbol{\sigma} \cdot \hat{\mathbf{q}} \hat{\mathbf{q}} \cdot \boldsymbol{\epsilon} \mathcal{F}_4 \quad (19)$$

and the  $\mathcal{F}_i$  are related to the  $A_i$  via

$$\begin{aligned} \mathcal{F}_1 &= (\sqrt{s} - M_N) \frac{N_1 N_2}{8\pi\sqrt{s}} \left[ A_1 + \frac{k \cdot q}{\sqrt{s} - M_N} A_3 + \left( \sqrt{s} - M_N - \frac{k \cdot q}{\sqrt{s} - M_N} \right) A_4 \right] \\ \mathcal{F}_2 &= (\sqrt{s} - M_N) \frac{N_1 N_2}{8\pi\sqrt{s}} \frac{|\mathbf{q}|}{E_2 + M_N} \\ &\quad \times \left[ -A_1 + \frac{k \cdot q}{\sqrt{s} + M_N} A_3 + \left( \sqrt{s} + M_N - \frac{k \cdot q}{\sqrt{s} + M_N} \right) A_4 \right] \\ \mathcal{F}_3 &= (\sqrt{s} - M_N) \frac{N_1 N_2}{8\pi\sqrt{s}} |\mathbf{q}| [ -(\sqrt{s} - M_N) A_2 + A_3 - A_4 ] \\ \mathcal{F}_4 &= (\sqrt{s} - M_N) \frac{N_1 N_2}{8\pi\sqrt{s}} \frac{|\mathbf{q}|^2}{E_2 + M_N} [ (\sqrt{s} + M_N) A_2 + A_3 - A_4 ] \end{aligned} \quad (20)$$

with

$$N_i = \sqrt{M_N + E_i}, \quad E_i = \sqrt{M_N^2 + \mathbf{p}_i^2}. \quad (21)$$

The projection matrix for the lowest multipoles  $E_{0+}$ ,  $M_{1+}$ ,  $M_{1-}$  and  $E_{1+}$  is given by

$$\begin{pmatrix} E_{0+} \\ M_{1+} \\ M_{1-} \\ E_{1+} \end{pmatrix} = \int_{-1}^1 dz \begin{pmatrix} \frac{1}{2}P_0 & -\frac{1}{2}P_1 & 0 & \frac{1}{6}[P_0 - P_2] \\ \frac{1}{4}P_1 & -\frac{1}{4}P_2 & \frac{1}{12}[P_2 - P_0] & 0 \\ -\frac{1}{2}P_1 & \frac{1}{2}P_0 & \frac{1}{6}[P_0 - P_2] & 0 \\ \frac{1}{4}P_1 & -\frac{1}{4}P_2 & \frac{1}{12}[P_0 - P_2] & \frac{1}{10}[P_1 - P_3] \end{pmatrix} \begin{pmatrix} \mathcal{F}_1 \\ \mathcal{F}_2 \\ \mathcal{F}_3 \\ \mathcal{F}_4 \end{pmatrix} \quad (22)$$

with  $P_i$  being the Legendre polynomials. Neglecting higher partial waves the differential cross section is given in terms of  $E_{0+}$ ,  $M_{1+}$ ,  $M_{1-}$  and  $E_{1+}$  by

$$\frac{|\mathbf{k}|}{|\mathbf{q}|} \frac{d\sigma}{d\Omega_{cm}} = A + B \cos \vartheta + C \cos^2 \vartheta, \quad (23)$$

with

$$\begin{aligned}
A &= |E_{0+}|^2 + |r|^2 \\
B &= 2\text{Re}(E_{0+}M_P^*) \\
C &= |M_P|^2 - |r|^2 \\
M_P &= 3E_{1+} + M_{1+} - M_{1-} \\
2|r|^2 &= |3E_{1+} - M_{1+} + M_{1-}|^2 + |2M_{1+} + M_{1-}|^2.
\end{aligned} \tag{24}$$

This completes the necessary formalism for the processes considered in this paper.

### 3 The effective Lagrangian

In this section, we will introduce the effective Lagrangian with  $\eta$  and  $\eta'$  coupled both to the ground state baryon octet and low-lying resonances in the  $s$ ,  $u$ - and  $t$ -channel. Recently, a systematic framework for the  $\eta'$  in baryon chiral perturbation theory has been developed [12]. Here, we will extend this formalism by including explicitly the low-lying meson and baryon resonances.

Our starting point is the  $U(3)_L \times U(3)_R$  chiral effective Lagrangian of the pseudoscalar meson nonet ( $\pi, K, \eta_8, \eta_0$ ) coupled to the ground state baryon octet ( $N, \Lambda, \Sigma, \Xi$ ) at lowest order in the derivative expansion

$$\mathcal{L} = \mathcal{L}_\phi + \mathcal{L}_{\phi B} \tag{25}$$

with

$$\mathcal{L}_\phi = -v_0\eta_0^2 + \frac{F_\pi^2}{4}\langle u_\mu u^\mu \rangle + \frac{F_\pi^2}{4}\langle \chi_+ \rangle + iF_0v_3\eta_0\langle \chi_- \rangle + \frac{1}{12}(F_0^2 - F_\pi^2)\langle u_\mu \rangle\langle u^\mu \rangle \tag{26}$$

and

$$\begin{aligned}
\mathcal{L}_{\phi B} &= i\langle \bar{B}\gamma_\mu[D^\mu, B] \rangle - M_N\langle \bar{B}B \rangle - \frac{1}{2}D\langle \bar{B}\gamma_\mu\gamma_5\{u^\mu, B\} \rangle \\
&\quad - \frac{1}{2}F\langle \bar{B}\gamma_\mu\gamma_5[u^\mu, B] \rangle - \lambda\langle \bar{B}\gamma_\mu\gamma_5B \rangle\langle u^\mu \rangle.
\end{aligned} \tag{27}$$

The pseudoscalar meson nonet is summarized in a matrix valued field  $U(x)$

$$U(\phi, \eta_0) = u^2(\phi, \eta_0) = \exp\left\{2i\phi/F_\pi + i\sqrt{\frac{2}{3}}\eta_0/F_0\right\}, \tag{28}$$

where  $F_\pi \simeq 92.4$  MeV is the pion decay constant and the singlet  $\eta_0$  couples to the singlet axial current with strength  $F_0$ . The unimodular part of the field  $U(x)$  contains the degrees of freedom of the Goldstone boson octet  $\phi$

$$\phi = \frac{1}{\sqrt{2}} \begin{pmatrix} \frac{1}{\sqrt{2}}\pi^0 + \frac{1}{\sqrt{6}}\eta_8 & \pi^+ & K^+ \\ \pi^- & -\frac{1}{\sqrt{2}}\pi^0 + \frac{1}{\sqrt{6}}\eta_8 & K^0 \\ K^- & \bar{K}^0 & -\frac{2}{\sqrt{6}}\eta_8 \end{pmatrix}, \tag{29}$$

while the phase  $\det U(x) = e^{i\sqrt{6}\eta_0/F_0}$  describes the  $\eta_0$ .<sup>3</sup> In order to incorporate the baryons into the effective theory it is convenient to form an object of axial-vector type with one derivative

$$u_\mu = iu^\dagger \nabla_\mu U u^\dagger \quad (30)$$

with  $\nabla_\mu$  being the covariant derivative of  $U$ . The expression  $\langle \dots \rangle$  denotes the trace in flavor space and the quark mass matrix  $\mathcal{M} = \text{diag}(m_u, m_d, m_s)$  enters in the combinations

$$\chi_\pm = 2B_0(u\mathcal{M}u \pm u^\dagger\mathcal{M}u^\dagger) \quad (31)$$

with  $B_0 = -\langle 0|\bar{q}q|0\rangle/F_\pi^2$  the order parameter of the spontaneous symmetry violation. Expanding the Lagrangian  $\mathcal{L}_\phi$  in terms of the meson fields one observes terms quadratic in the meson fields that contain the factor  $\eta_0\eta_8$  which leads to  $\eta_0$ - $\eta_8$  mixing. Such terms arise from the explicitly symmetry breaking terms  $\frac{F_\pi^2}{4}\langle\chi_+\rangle + iF_0v_3\eta_0\langle\chi_-\rangle$  and read

$$-\left(\frac{2\sqrt{2}F_\pi}{3}\frac{F_\pi}{F_0} + \frac{8}{\sqrt{3}}\frac{F_0}{F_\pi}v_3\right)B_0(\hat{m} - m_s)\eta_0\eta_8 \quad (32)$$

with  $\hat{m} = \frac{1}{2}(m_u + m_d)$ . The states  $\eta_0$  and  $\eta_8$  are therefore not mass eigenstates. The mixing yields the eigenstates  $\eta$  and  $\eta'$ ,

$$\begin{aligned} |\eta\rangle &= \cos\theta|\eta_8\rangle - \sin\theta|\eta_0\rangle \\ |\eta'\rangle &= \sin\theta|\eta_8\rangle + \cos\theta|\eta_0\rangle, \end{aligned} \quad (33)$$

which is valid in the leading order of flavor symmetry breaking and we have neglected other pseudoscalar isoscalar states which could mix with both  $\eta_0$  and  $\eta_8$ . The  $\eta$ - $\eta'$  mixing angle can be determined from the two photon decays of  $\pi^0, \eta, \eta'$ , which require a mixing angle around  $-20^\circ$  [13]. We will make use of this experimental input in order to diagonalize the mass terms of the effective mesonic Lagrangian.

The baryonic Lagrangian consists of the free kinetic term and the axial-vector couplings of the mesons to the baryons. The values of the LECs  $D$  and  $F$  can be extracted from semileptonic hyperon decays. A fit to the experimental data delivers  $D = 0.80 \pm 0.01$  and  $F = 0.46 \pm 0.01$  [14]. We leave the third axial-vector coupling  $\lambda$  undetermined for the time being. The covariant derivative of the baryon field is given by

$$[D_\mu, B] = \partial_\mu B + [\Gamma_\mu, B] \quad (34)$$

with the chiral connection

$$\Gamma_\mu \simeq -iv_\mu = ieQ\mathcal{A}_\mu \quad (35)$$

---

<sup>3</sup>For details the reader is referred to [12].

to the order we are working and  $Q = \frac{1}{3}\text{diag}(2, -1, -1)$  is the quark charge matrix. Note that there is no pseudoscalar coupling of  $\eta_0$  to the baryons of the form  $\eta_0 \bar{B} \gamma_5 B$ . Such a term is in principle possible but can be absorbed by the  $\lambda$ -term in Eq. (27) by means of the equation of motion for the baryons. Since we confine ourselves to the lowest order Lagrangian for the ground state baryon octet, higher order terms are omitted. The main purpose here is to investigate the importance of lowest order Born terms and resonance exchange. In order to obtain an improved description one must, of course, include higher order counterterms such as the anomalous magnetic moments of the nucleons.

We now proceed by including explicitly low-lying resonances in our theory. In the  $t$ -channel the lowest-lying resonances are the nonet of the vector mesons ( $\rho, K^*, \omega_8, \omega_0$ ). According to [9] no evidence for  $\rho$  and  $\omega$  exchange in the  $t$ -channel is given. We will investigate this statement within our framework. The vector mesons couple in a chiral invariant way to the baryons and the pseudoscalar mesons via the Lagrangian

$$\mathcal{L} = \mathcal{L}_{VBB} + \mathcal{L}_{V\gamma\phi} \quad (36)$$

with

$$\mathcal{L}_{VBB} = g_{VBB}^D \langle \bar{B} \Gamma_\mu \{V^\mu, B\} \rangle + g_{VBB}^F \langle \bar{B} \Gamma_\mu [V^\mu, B] \rangle + g_{VBB}^0 \omega_\mu^0 \langle \bar{B} \Gamma_\mu B \rangle, \quad (37)$$

where the operator  $\Gamma_\mu$  involves a vector and a tensor coupling

$$\Gamma_\mu = \gamma_\mu + i \frac{\kappa_V}{2M_N} \sigma_{\mu\nu} (p' - p)^\nu. \quad (38)$$

The electromagnetic piece of the Lagrangian is given by

$$\mathcal{L}_{V\gamma\phi} = -g_{V\gamma\phi}^8 \epsilon^{\mu\nu\alpha\beta} \langle V_\mu \{u_\nu, F_{\alpha\beta}^+\} \rangle - g_{V\gamma\phi}^0 \epsilon^{\mu\nu\alpha\beta} \omega_\mu^0 \langle u_\nu F_{\alpha\beta}^+ \rangle. \quad (39)$$

The quantity  $F_{\alpha\beta}^+$  contains the electromagnetic field strength tensor  $F_{\alpha\beta}$  of  $v_\mu$

$$\begin{aligned} F_{\alpha\beta}^+ &\equiv u^\dagger F_{\alpha\beta} u + u F_{\alpha\beta} u^\dagger \\ &= 2(\partial_\alpha v_\beta - \partial_\beta v_\alpha) + \mathcal{O}(\phi^2). \end{aligned} \quad (40)$$

The states  $\omega_8$  and  $\omega_0$  mix to yield the physical states  $\omega$  and  $\phi$ . The mixing is characterized by the angle  $\varphi$

$$\begin{aligned} |\omega\rangle &= \cos \varphi |\omega_8\rangle - \sin \varphi |\omega_0\rangle \\ |\phi\rangle &= \sin \varphi |\omega_8\rangle + \cos \varphi |\omega_0\rangle \end{aligned} \quad (41)$$

with  $\varphi \simeq 40^\circ$  [15]. The LECs of the effective Lagrangian are usually expressed in terms of the physical couplings  $g_{VN}$  of  $\rho_0, \omega$  and  $\phi$  to the proton

$$\mathcal{L}_{Vpp} = \frac{1}{2} \bar{p} \Gamma_\mu p \sum_{V=\rho_0, \omega, \phi} g_{VN} V^\mu. \quad (42)$$

Comparison with the Lagrangian in Eq. (37) leads to

$$\begin{aligned}
g_{VBB}^D &= \frac{\sqrt{3}}{4\sqrt{2}} \left[ \sqrt{3}g_{\rho N} - \cos\varphi g_{\omega N} - \sin\varphi g_{\phi N} \right] \\
g_{VBB}^F &= \frac{\sqrt{3}}{4\sqrt{2}} \left[ \frac{1}{\sqrt{3}}g_{\rho N} + \cos\varphi g_{\omega N} + \sin\varphi g_{\phi N} \right] \\
g_{VBB}^0 &= \frac{1}{2} \left[ \cos\varphi g_{\phi N} - \sin\varphi g_{\omega N} \right].
\end{aligned} \tag{43}$$

It follows immediately, that the coupling of  $\rho_0, \omega$  and  $\phi$  to the neutron is given by

$$\mathcal{L}_{Vnn} = \frac{1}{2} \bar{n} \Gamma_\mu n \left( -g_{\rho N} \rho_0^\mu + g_{\omega N} \omega^\mu + g_{\phi N} \phi^\mu \right). \tag{44}$$

The couplings  $g_{VN}$  are quite well known, we use  $g_{\rho N} = 6.08$  and  $g_{\omega N} = 3g_{\rho N}$  [16]. The  $g_{\phi N}$  coupling turns out to be much smaller than  $g_{\omega N}$  [15] (in agreement with the OZI suppression), so we can safely neglect the  $\phi$  meson in our calculations by setting  $g_{\phi N} = 0$ . Furthermore, the tensor coupling for the  $\rho$  meson is given by  $\kappa_\rho = 6$ , whereas  $\kappa_\omega \simeq 0$ . Instead of using a common tensor coupling  $\kappa_V$  for  $\rho$  and  $\omega$ , as prescribed by the Lagrangian in Eq. (37), we prefer to work with the physical values  $\kappa_\rho = 6$  and  $\kappa_\omega = 0$ .

We proceed in a similar manner with the electromagnetic piece of the Lagrangian by defining the physical couplings

$$\mathcal{L}_{V\gamma\phi} = e \epsilon^{\mu\nu\alpha\beta} \partial_\alpha \mathcal{A}_\beta \left( \partial_\nu \eta \sum_{V=\rho_0, \omega, \phi} g_{V\gamma\eta} V_\mu + \partial_\nu \eta' \sum_{V=\rho_0, \omega, \phi} g_{V\gamma\eta'} V_\mu \right) \tag{45}$$

which are related to the  $SU(3)$  couplings via

$$\begin{aligned}
g_{V\gamma\phi}^8 &= \left[ \frac{8}{\sqrt{3}F_0} \sin\theta - 4\sqrt{\frac{2}{3}} \frac{1}{F_\pi} \cos\theta \right]^{-1} g_{\rho\gamma\eta} \\
g_{V\gamma\phi}^0 &= \frac{\sqrt{3}F_\pi}{4 \cos\theta} \left[ \sin\varphi g_{\omega\gamma\eta} - \cos\varphi g_{\phi\gamma\eta} \right].
\end{aligned} \tag{46}$$

The experimental values for the  $g_{V\gamma\eta}$  can be extracted from the decay width of radiative decays of the vector mesons

$$\Gamma(V \rightarrow \eta\gamma) = \frac{e^2}{96\pi} g_{V\gamma\eta}^2 \left( m_V - \frac{m_\eta^2}{m_V} \right)^3. \tag{47}$$

Using the values for  $\Gamma(\rho \rightarrow \eta\gamma)$  and  $\Gamma(\omega \rightarrow \eta\gamma)$  from [13] we obtain

$$\begin{aligned}
g_{\rho\gamma\eta} &= 1.8 \text{ GeV}^{-1} \\
g_{\omega\gamma\eta} &= 0.23 \text{ GeV}^{-1}.
\end{aligned} \tag{48}$$

Once the couplings of the vector mesons with  $\eta$  have been determined, their coupling strength to  $\eta'$  could in principle be calculated by making use of the

Lagrangian in Eq. (39). But in order to get a more accurate estimate of these couplings, it is preferable to extract the coupling constants  $g_{\rho\gamma\eta'}$  and  $g_{\omega\gamma\eta'}$  directly from the decay widths of the pertinent radiative decays

$$\Gamma(\eta' \rightarrow V\gamma) = \frac{e^2}{32\pi} g_{V\gamma\eta'}^2 (m_{\eta'} - \frac{m_V^2}{m_{\eta'}})^3. \quad (49)$$

We obtain

$$\begin{aligned} g_{\rho\gamma\eta'} &= 1.31 \text{ GeV}^{-1} \\ g_{\omega\gamma\eta'} &= 0.45 \text{ GeV}^{-1}. \end{aligned} \quad (50)$$

This determines completely the contributions of the vector mesons. Note that the vector meson contribution is usually reduced, e.g., by using a form factor [7]. However, this effect should be reasonably small for  $\eta$  and  $\eta'$  photoproduction close to threshold.

Baryon resonances contribute in the  $s$ - and  $u$ -channel. In this work we consider the lowest-lying  $S$ - and  $P$ -wave baryon resonances, i.e. the  $J^P = 1/2^+$  and  $1/2^-$  octets which include  $P_{11}(1440)$  and  $S_{11}(1535)$ , respectively. We will neglect higher partial waves baryon resonances such as  $D_{13}(1520)$ . Both  $P_{11}(1440)$  and  $S_{11}(1535)$  contribute to  $\eta$  photoproduction and experimental dominance of  $S_{11}(1535)$  is found [1]. On the other hand, the situation for  $\eta'$  photoproduction is not so clear. It has been discussed in the literature whether the data for  $\eta'$  photoproduction on the proton can be understood by taking resonances in the 2 GeV region or off-shell effects of  $S_{11}(1535)$  into account [7, 8]. In the present investigation we will extend the formalism for the chiral  $U(3)$  Lagrangian presented in [12] by including the  $J^P = 1/2^+$  and  $1/2^-$  baryon resonance octets. As we will see shortly, the parameters of such a Lagrangian can be fixed from strong and radiative decays of the resonances. This allows us to predict the contributions of  $P_{11}(1440)$  and  $S_{11}(1535)$  both for  $\eta$  and  $\eta'$  photoproduction. Within our effective Lagrangian approach the results will be predictive and no additional parameters have to be fitted to obtain agreement with experiment. Therefore, the application of the  $U(3)$  formalism within baryon chiral perturbation theory to photoproduction processes is a highly nontrivial check of this method. It can also clarify the importance of the  $S_{11}(1535)$  resonance for  $\eta'$  photoproduction. To this end, it is sufficient to obtain a rough estimate for the resonance contributions. In order to achieve better agreement with experiment, one has to consider further resonances, e.g.  $D_{13}(1520)$  and  $S_{11}(1650)$ , and include chiral loop corrections. But this is beyond the scope of the present investigation and the calculations are performed at tree level.

Let us first consider the spin- $1/2^+$  octet which we denote by  $P$ . The octet consists of  $N^*(1440)$ ,  $\Sigma^*(1660)$ ,  $\Lambda^*(1600)$ ,  $\Xi^*(?)$  and the effective Lagrangian of the  $P$ -wave octet coupled to the ground state baryon octet takes the form

$$\mathcal{L} = \mathcal{L}_P + \mathcal{L}_{\phi BP} \quad (51)$$

with the kinetic term

$$\mathcal{L}_P = i\langle\bar{P}\gamma_\mu[D^\mu, P]\rangle - M_P\langle\bar{P}P\rangle. \quad (52)$$

Since for the processes considered here only  $N^*(1440)$  contributes, we set  $M_P = 1.44$  GeV. The interaction terms of the  $P$ -wave resonances with the ground state baryon octet read

$$\begin{aligned} \mathcal{L}_{\phi BP} = & -\frac{1}{2}D_P\langle\bar{P}\gamma_\mu\gamma_5\{u^\mu, B\}\rangle - \frac{1}{2}F_P\langle\bar{P}\gamma_\mu\gamma_5[u^\mu, B]\rangle - \lambda_P\langle\bar{P}\gamma_\mu\gamma_5 B\rangle\langle u^\mu\rangle \\ & + d_P\langle\bar{P}\sigma^{\mu\nu}\{F_{\mu\nu}^+, B\}\rangle + f_P\langle\bar{P}\sigma^{\mu\nu}[F_{\mu\nu}^+, B]\rangle + \text{h.c.} . \end{aligned} \quad (53)$$

A possible  $\eta_0\bar{P}\gamma_5 B$  term can again be eliminated by using the equation of motion for baryons. The coupling constants  $D_P, F_P$  and  $d_P, f_P$  can be determined from strong and radiative decays of the  $N^*(1440)$  resonance, cf. App. A; we use the central values

$$\begin{aligned} D_P &= 0.32, & F_P &= 0.16 \\ d_P &= -0.05 \text{ GeV}^{-1}, & f_P &= 0.08 \text{ GeV}^{-1}. \end{aligned} \quad (54)$$

The spin-1/2<sup>-</sup> octet consists of  $N^*(1535), \Lambda^*(1670), \Sigma^*(1750), \Xi^*(?)$  and the pertinent Lagrangian reads

$$\mathcal{L} = \mathcal{L}_S + \mathcal{L}_{\phi BS} \quad (55)$$

with the kinetic term

$$\mathcal{L}_S = i\langle\bar{S}\gamma_\mu[D^\mu, S]\rangle - M_S\langle\bar{S}S\rangle \quad (56)$$

and the interaction part

$$\begin{aligned} \mathcal{L}_{\phi BS} = & -\frac{i}{2}D_S\langle\bar{S}\gamma_\mu\{u^\mu, B\}\rangle - \frac{i}{2}F_S\langle\bar{S}\gamma_\mu[u^\mu, B]\rangle - i\lambda_S\langle\bar{S}\gamma_\mu B\rangle\langle u^\mu\rangle \\ & + id_S\langle\bar{S}\sigma^{\mu\nu}\gamma_5\{F_{\mu\nu}^+, B\}\rangle + if_S\langle\bar{S}\sigma^{\mu\nu}\gamma_5[F_{\mu\nu}^+, B]\rangle + \text{h.c.} . \end{aligned} \quad (57)$$

We set  $M_S = 1.535$  GeV and from strong and radiative decays of the  $S$ -wave resonances one obtains, cf. App. A,

$$\begin{aligned} D_S &= 0.37, & F_S &= -0.21, & \lambda_S &= -0.07 \\ d_S &= -0.07 \text{ GeV}^{-1}, & f_S &= -0.06 \text{ GeV}^{-1}. \end{aligned} \quad (58)$$

Since there exists data on decay channels of the  $S$ -wave resonances into  $\eta$ , we are able to fix the coupling  $\lambda_S$  by taking  $\eta$ - $\eta'$  mixing into account, whereas for  $\lambda_P$  we relegate the discussion to Sec. 5. Several remarks are in order. First, we would like to point out that our simple ansatz of zero width resonances will lead to singularities at the resonance mass which could be circumvented by the use of a finite width. This will restrict in the case of  $\eta$  photoproduction the validity of our approach to energies very close to threshold which we are considering

in the present work, whereas it is numerically irrelevant for  $\eta'$  photoproduction. Furthermore, the couplings of the resonances to the nucleons are determined by their pertinent decay widths. Therefore, their sign is not fixed and a different choice of their signs leads to changes in our results. We have chosen the signs of the resonance couplings in such a way, that they lead to better agreement with existing data for  $\eta$  and  $\eta'$  photoproduction and do not present the results for the other possible values of the couplings. Finally, we have calculated both Born terms using the lowest order chiral effective Lagrangian and resonance contributions. We would like to emphasize that this procedure does not imply any double counting. The contributions of the resonances are hidden only in higher chiral order counterterms of the effective Lagrangian which we did not take into account in the present investigation. Born terms like the ones used in this work are not produced by resonance contributions.

## 4 Invariant amplitudes

We proceed by presenting the invariant amplitudes for  $\eta$  and  $\eta'$  photoproduction on the nucleons. Let us start with the Born terms which vanish in the case of the neutron. The diagrams contributing to photoproduction off the proton are depicted in Fig. 1 and they read

$$\begin{aligned}
A_1(p\gamma \rightarrow p\phi) &= -2M_N e A_\phi \left[ \frac{1}{s - M_N^2} + \frac{1}{u - M_N^2} \right] \\
A_2(p\gamma \rightarrow p\phi) &= 4M_N e A_\phi \frac{1}{[s - M_N^2][u - M_N^2]} \\
A_3(p\gamma \rightarrow p\phi) &= A_4(p\gamma \rightarrow p\phi) = 0
\end{aligned} \tag{59}$$

with

$$\begin{aligned}
A_\eta &= \frac{1}{2\sqrt{3}F_\pi} [D - 3F] \cos \theta + \sqrt{\frac{2}{3}} \frac{1}{F_0} [D + 3\lambda] \sin \theta \\
A_{\eta'} &= \frac{1}{2\sqrt{3}F_\pi} [D - 3F] \sin \theta - \sqrt{\frac{2}{3}} \frac{1}{F_0} [D + 3\lambda] \cos \theta.
\end{aligned} \tag{60}$$

This leads to the total cross section

$$\begin{aligned}
\sigma_{tot}(p\gamma \rightarrow p\phi) &= -\frac{\lambda^{1/2}(s, M_N^2, m_\phi^2)}{4\pi s [s - M_N^2]} M_N^2 e^2 A_\phi^2 \left( \frac{1}{2s} [3s - M_N^2 + m_\phi^2] \right. \\
&\quad - \frac{4sm_\phi^2}{[s - M_N^2]^2} - \frac{4s}{\Delta_\phi} \left[ \frac{1}{2} - m_\phi^2 \frac{s + M_N^2 - m_\phi^2}{[s - M_N^2]^2} \right] \\
&\quad \left. \times \ln \left[ \frac{s + M_N^2 - m_\phi^2 + \Delta_\phi}{2\sqrt{s}M_N} \right] \right)
\end{aligned} \tag{61}$$

with

$$\Delta_\phi = \sqrt{(s - M_N^2 + m_\phi^2)^2 - 4sm_\phi^2}. \quad (62)$$

Vector meson exchange is shown in Fig. 2. One has to add the following terms to the invariant amplitudes for photoproduction on the proton

$$\begin{aligned} A_1(p\gamma \rightarrow p\phi) &= \frac{e\kappa_\rho}{4M_N} g_{\rho N} g_{\rho\gamma\phi} \frac{t}{t - M_\rho^2} \\ A_2(p\gamma \rightarrow p\phi) &= \frac{e\kappa_\rho}{4M_N} g_{\rho N} g_{\rho\gamma\phi} \frac{1}{t - M_\rho^2} \\ A_3(p\gamma \rightarrow p\phi) &= 0 \\ A_4(p\gamma \rightarrow p\phi) &= -\frac{e}{2} \sum_{V=\rho_0,\omega,\phi} g_{VN} g_{V\gamma\phi} \frac{1}{t - M_V^2}. \end{aligned} \quad (63)$$

For the neutron  $g_{\rho N}$  has to be replaced by  $-g_{\rho N}$ .

We now turn to the baryon resonances. Their contributions are given in Fig. 3 and read for the spin-1/2<sup>+</sup> octet in the proton case

$$\begin{aligned} A_1(p\gamma \rightarrow p\phi) &= -e\frac{4}{3}(d_P + 3f_P)P_\phi \left[ \frac{u - M_N^2}{u - M_P^2} + \frac{s - M_N^2}{s - M_P^2} \right] \\ A_2(p\gamma \rightarrow p\phi) &= 0 \\ A_3(p\gamma \rightarrow p\phi) &= e\frac{4}{3}(d_P + 3f_P)P_\phi(M_P + M_N) \left[ \frac{1}{s - M_P^2} - \frac{1}{u - M_P^2} \right] \\ A_4(p\gamma \rightarrow p\phi) &= e\frac{4}{3}(d_P + 3f_P)P_\phi(M_P + M_N) \left[ \frac{1}{s - M_P^2} + \frac{1}{u - M_P^2} \right] \end{aligned} \quad (64)$$

with

$$\begin{aligned} P_\eta &= \frac{1}{2\sqrt{3}F_\pi} [D_P - 3F_P] \cos \theta + \sqrt{\frac{2}{3}} \frac{1}{F_0} [D_P + 3\lambda_P] \sin \theta \\ P_{\eta'} &= \frac{1}{2\sqrt{3}F_\pi} [D_P - 3F_P] \sin \theta - \sqrt{\frac{2}{3}} \frac{1}{F_0} [D_P + 3\lambda_P] \cos \theta, \end{aligned} \quad (65)$$

whereas the results for the neutron are obtained by replacing  $d_P + 3f_P$  by  $-2d_P$  in Eq. (64). The contributions from the spin-1/2<sup>-</sup> resonances read in the case of the proton

$$\begin{aligned} A_1(p\gamma \rightarrow p\phi) &= e\frac{4}{3}(d_S + 3f_S)S_\phi \left[ \frac{u - M_N^2}{u - M_S^2} + \frac{s - M_N^2}{s - M_S^2} \right] \\ A_2(p\gamma \rightarrow p\phi) &= 0 \\ A_3(p\gamma \rightarrow p\phi) &= e\frac{4}{3}(d_S + 3f_S)S_\phi(M_S - M_N) \left[ \frac{1}{s - M_S^2} - \frac{1}{u - M_S^2} \right] \\ A_4(p\gamma \rightarrow p\phi) &= e\frac{4}{3}(d_S + 3f_S)S_\phi(M_S - M_N) \left[ \frac{1}{s - M_S^2} + \frac{1}{u - M_S^2} \right] \end{aligned} \quad (66)$$

with

$$\begin{aligned}
S_\eta &= \frac{1}{2\sqrt{3}F_\pi}[D_S - 3F_S] \cos \theta + \sqrt{\frac{2}{3}} \frac{1}{F_0}[D_S + 3\lambda_S] \sin \theta \\
S_{\eta'} &= \frac{1}{2\sqrt{3}F_\pi}[D_S - 3F_S] \sin \theta - \sqrt{\frac{2}{3}} \frac{1}{F_0}[D_S + 3\lambda_S] \cos \theta,
\end{aligned} \tag{67}$$

where for neutrons  $d_S + 3f_S$  in Eq. (66) has to be replaced by  $-2d_S$ .

## 5 Numerical results

In this section, we discuss the numerical results for the central values of the resonance couplings as given in Sec. 3. We were able to determine most LECs by using experimental data from both semileptonic decays of the ground state baryon octet and from strong and radiative decays of the baryon resonances. The coupling constants of the vector meson Lagrangian are quite well known. The only parameters not fixed so far are the couplings  $\lambda$  and  $\lambda_P$  of the axial flavor-singlet baryonic currents. We note that from large  $N_c$  counting rules, one expects  $|\lambda| < |D|, |F|$  and  $|\lambda_P| < |D_P|, |F_P|$ . In order to get an estimate of these couplings we therefore varied their values within a small range around zero. It turns out that the dependence on  $\lambda_P$  is almost negligible and one can safely set  $\lambda_P = 0$ . Variation of  $\lambda$  leads to some smaller changes in the results and we find improved agreement with experiment for  $\lambda = 0.05$ . Of course, we could achieve better agreement with experiment by fine-tuning all parameters, but here we are only interested in a rough estimate of the resonance contributions. For  $F_0$  we employ the large  $N_c$  identity  $F_0 = F_\pi$ . Once the parameters are determined, the resonance contributions are fixed both for  $\eta$  and  $\eta'$  photoproduction. This will particularly clarify the importance of low-lying resonances for  $\eta'$  photoproduction within the chiral  $U(3)$  Lagrangian approach presented in this paper, since our results are predictions rather than a fit to experimental data. It also serves as a check if the  $\eta'$  can in general be included in baryon chiral perturbation theory in a systematic fashion as proposed in [12].

In Fig. 4 we present the total cross sections obtained from our tree level model. We restrict ourselves to the threshold region, since chiral loop effects and contributions from further resonances will become more important with increasing c.m. energy  $s$ . We are able to achieve reasonable agreement with existing data. However, the energy bins of the experiment for  $\eta'$  photoproduction on the proton are 100 MeV and 200 MeV wide [9] and can therefore not be compared directly with our theoretical estimates. But we obtain a total cross section for  $\eta'$  photoproduction which is in the same order of magnitude as in the experiment, i.e.  $\simeq 1.5 \mu\text{b}$ . In particular,  $\eta'$  photoproduction close to threshold can be understood without taking any further resonances into account. The dashed lines

in Fig. 4 are the contributions from the Born terms without the inclusion of resonances. Obviously, the resonances considered in this model lead to sizeable contributions except for  $\eta'$  photoproduction on the proton in which case the sum of their contributions is almost negligible. Furthermore, we are able to reproduce the ratio of  $\eta$  photoproduction on the neutron and the proton, which is experimentally found to be  $2/3$  [10]. It is also worthwhile to compare our results for the differential cross sections with experimental data. In Fig. 5 we show the differential cross sections for  $\eta$  and  $\eta'$  photoproduction on the proton close to threshold. The data for  $\eta'$  photoproduction as shown in Fig. 5b) is the energy-integrated angular distribution for  $1.44 \text{ GeV} < E_\gamma < 1.54 \text{ GeV}$ . Dividing by the phase space factor  $|\mathbf{q}|/|\mathbf{k}|$  in Eq. (6) in order to account for the wide energy bin one obtains experimental data which have a slightly smaller differential cross section than obtained in our model. This might indicate that we overestimated the resonances, e.g., by not using a form factor for the vector mesons. Nevertheless, our simplified treatment of  $\eta$  and  $\eta'$  photoproduction shows, that one is able to understand the size of experimental data just by considering lowest order Born terms and resonance exchange.

In Figs. 6 and 7 we present the results for the multipoles  $E_{0+}$ ,  $M_{1+}$ ,  $M_{1-}$  and  $E_{1+}$  in the threshold region. In order to estimate the significance of the different resonances, we show in Table 1 the multipoles for  $\eta$  photoproduction off the proton at c.m. energy  $s = 708 \text{ MeV}$  both with and without resonances. We conclude that while the spin- $1/2^+$  resonance octet does not contribute significantly, both vector mesons and spin- $1/2^-$  octet lead to sizeable contributions. For completeness we present the energy dependence of the coefficients  $A$ ,  $B$  and  $C$  from Eq. (23) in Figs. 8 and 9.

## 6 Summary

In the present work, we studied  $\eta$  and  $\eta'$  photoproduction on both the proton and neutron. To this end, we pinned down an effective chiral  $U(3)$  Lagrangian which describes the interactions of the pseudoscalar meson nonet ( $\pi, K, \eta, \eta'$ ) with the ground state baryon octet and low-lying resonances. These include the vector mesons  $\rho_0$  and  $\omega$  in the  $t$ -channel (the  $\phi$  meson leads to much smaller contributions and can be neglected for our purposes), and the  $J^P = 1/2^+$  and  $1/2^-$  baryon resonances  $P_{11}(1440)$  and  $S_{11}(1535)$ . Our aim here is to obtain a rough estimate of the contributions of these low-lying resonances both for  $\eta$  and  $\eta'$  photoproduction. Further resonances have therefore been neglected, such as  $S_{11}(1650)$  and the higher partial wave resonance  $D_{13}(1520)$ .

Most LECs of the effective Lagrangian can be determined using semileptonic hyperon decays and both strong and radiative decays of the baryon resonances. The couplings of the vector mesons are also quite well known. Only the couplings of the axial flavor-singlet currents of the ground state and spin- $1/2^+$  resonance

baryons,  $\lambda$  and  $\lambda_P$ , could not be fixed from experiment. Variation of both parameters within a realistic range revealed that  $\lambda_P$  does almost not alter our results and is therefore set to zero. For  $\lambda$  we have chosen a value which leads to improved agreement with experiment. Our results are therefore predictions rather than fits to experiment.

We calculated the Born terms and the resonance contributions to  $\eta$  and  $\eta'$  photoproduction on the nucleons using the chiral  $U(3)$  Lagrangian. Comparison with data close to threshold shows that this simple model is capable of producing simultaneously reasonable agreement with  $\eta$  and  $\eta'$  photoproduction both on the neutron and proton, i.e. the size of the experimental data for photoproduction of the  $\eta'$  meson can be understood just by taking low-lying resonances into account. Of course, we do not expect our model to be valid for higher c.m. energies away from threshold, since other effects such as contributions from further resonances and chiral loop corrections will become significant. We are able to reproduce the ratio of  $\eta$  photoproduction on the neutron and the proton, which is experimentally found to be  $2/3$  [1]. Reasonable agreement with experiment is also obtained for the differential cross sections, which is almost constant for  $\eta$  photoproduction and forward-peaked in the case of  $\eta'$ . Finally, we present results for the multipole decomposition of  $\eta$  photoproduction. Within our model, we find, that contributions from vector mesons and  $S_{11}(1535)$  dominate, whereas contributions from  $P_{11}(1440)$  lead to some minor corrections.

The present investigation also served as a check if the  $\eta'$  meson can be included in baryon chiral perturbation theory as proposed in [12]. The findings of the present investigation concerning  $\eta'$  photoproduction can be confirmed, e.g., by employing the chiral  $U(3)$  meson-baryon Lagrangian without explicit resonances in a coupled channel approach. This will generate dynamically the baryon resonances as was shown in [5] for  $\eta$  photoproduction. Work on this subject is currently underway.

## Acknowledgments

The author wishes to thank N. Kaiser for useful discussions and suggestions.

## A Determination of the baryon resonance couplings

In order to determine the strong coupling constants of the baryon resonances, we use the decays  $N^*(1440) \rightarrow N\pi$ ,  $\Lambda^*(1600) \rightarrow \Sigma\pi$  and  $N^*(1535) \rightarrow N\pi$ ,  $N^*(1535) \rightarrow N\eta$ ,  $\Lambda^*(1670) \rightarrow \Lambda\eta$ , see also [17]. The width follows via

$$\Gamma = \frac{1}{8\pi M_R^2} |\mathbf{q}_\phi| |\mathcal{T}|^2 \quad (\text{A.1})$$

with

$$|\mathbf{q}_\phi| = \frac{1}{2M_R} \left[ (M_R^2 - (M_B + m_\phi)^2) (M_R^2 - (M_B - m_\phi)^2) \right]^{1/2} \quad (\text{A.2})$$

being the three-momentum of the meson  $\phi = \pi, \eta$  in the rest frame of the resonance. The terms  $M_R$  and  $M_B$  are the masses of the resonance and the ground state baryon, respectively. We employ the physical masses of the baryons involved in a decay. The mistake we make in not using common octet masses is of higher chiral order and, therefore, beyond the accuracy of our calculation. For the transition matrix one obtains in the case of  $P$ -wave resonances

$$|\mathcal{T}|^2 = \frac{1}{2F_\pi^2} (M_R + M_B)^2 \left[ (M_R - M_B)^2 - m_\phi^2 \right] A_{P\phi} \quad (\text{A.3})$$

and for the  $S$ -waves

$$|\mathcal{T}|^2 = \frac{1}{2F_\pi^2} (M_R - M_B)^2 \left[ (M_R + M_B)^2 - m_\phi^2 \right] A_{S\phi} \quad (\text{A.4})$$

with the coefficients

$$\begin{aligned} A_{N^*(1440)\pi} &= \frac{3}{2} (D_P + F_P)^2, & A_{\Lambda^*(1600)\pi} &= 2D_P^2, & A_{N^*(1535)\pi} &= \frac{3}{2} (D_S + F_S)^2, \\ A_{N^*(1535)\eta} &= \frac{1}{6} \left[ (D_S - 3F_S) \cos \theta + \sqrt{8} \frac{F_\pi}{F_0} (D_S + 3\lambda_S) \sin \theta \right]^2, \\ A_{\Lambda^*(1670)\eta} &= \frac{2}{3} \left[ D_S \cos \theta + \sqrt{2} \frac{F_\pi}{F_0} (D_S + 3\lambda_S) \sin \theta \right]^2 \end{aligned} \quad (\text{A.5})$$

where we have taken  $\eta$ - $\eta'$  mixing into account. For  $F_0$  we employ the large  $N_c$  value  $F_0 = F_\pi$ . Using the experimental values for the decay widths we arrive at the central values

$$\begin{aligned} D_P &= 0.32, & F_P &= 0.16 \\ D_S &= 0.37, & F_S &= -0.21, & \lambda_S &= -0.07 \end{aligned} \quad (\text{A.6})$$

where we have chosen the signs in accordance with the data for  $\eta$  and  $\eta'$  photoproduction. We do not present the uncertainties in these parameters here, since for the purpose of our considerations a rough estimate of these constants is sufficient.

We now turn to the determination of the couplings  $d_P, f_P$  and  $d_S, f_S$  appearing in the electromagnetic part of the effective resonance-ground state Lagrangian. The decays listed in the particle data book, which determine the coupling constants  $d_S$  and  $f_S$ , are  $N^*(1535) \rightarrow N\gamma$ , see also [18]. The width is given by

$$\Gamma^{ji} = \frac{1}{8\pi M_S^2} |\mathbf{k}_\gamma| |\mathcal{T}^{ji}|^2 \quad (\text{A.7})$$

with

$$|\mathbf{k}_\gamma| = E_\gamma = \frac{1}{2M_S} (M_S^2 - M_B^2) \quad (\text{A.8})$$

being the three-momentum of the photon in the rest frame of the resonance. For the transition matrix one obtains

$$|\mathcal{T}^{ji}|^2 = 128 e^2 (p_i \cdot k)^2 (C^{ji})^2 \quad (\text{A.9})$$

with  $p_i$  the momentum of the decaying baryon and the coefficients

$$C^{p^*(1535)p} = \frac{1}{3} d_S + f_S, \quad C^{n^*(1535)n} = -\frac{2}{3} d_S \quad . \quad (\text{A.10})$$

Using the experimental values for the decay widths we arrive at the central values

$$d_S = -0.07 \text{ GeV}^{-1}, \quad f_S = -0.06 \text{ GeV}^{-1}. \quad (\text{A.11})$$

For the determination of  $d_P$  and  $f_P$  we use the decays  $N^*(1440) \rightarrow N\gamma$ . One has to replace the resonance mass by  $M_P \simeq 1440 \text{ MeV}$  in Eq. (A.7,A.8) and the coefficients read

$$C^{p^*(1440)p} = \frac{1}{3} d_P + f_P, \quad C^{n^*(1440)n} = -\frac{2}{3} d_P. \quad (\text{A.12})$$

The fit to the decay widths delivers

$$d_P = -0.05 \text{ GeV}^{-1}, \quad f_P = 0.08 \text{ GeV}^{-1}. \quad (\text{A.13})$$

## References

- [1] B. Krusche et al., Phys. Rev. Lett. **74** (1995) 3736
- [2] M. Benmerrouche, N. C. Mukhopadhyay, Phys. Rev. Lett. **67** (1991) 1070;  
M. Benmerrouche, N. C. Mukhopadhyay, J. F. Zhang, Phys. Rev. **D51**  
(1995) 3237
- [3] C. Bennhold, H. Tanabe, Nucl. Phys. **A530** (1991) 625
- [4] L. Tiator, C. Bennhold, S.S. Kamalov, Nucl. Phys. **A580** (1994) 455
- [5] N. Kaiser, T. Waas, W. Weise, Nucl. Phys. **A612** (1997) 297;  
J. Caro Ramon, N. Kaiser, S. Wetzell, W. Weise, Nucl. Phys. **A672** (2000)  
249
- [6] S. Weinberg, Phys. Rev. **D11** (1975) 3583
- [7] J. F. Zhang, N. C. Mukhopadhyay, M. Benmerrouche, Phys. Rev. **C52**  
(1995) 1134
- [8] Z. Li, J. Phys. **G23** (1997) 1127

- [9] R. Plötzke et al., Phys. Lett. **B444** (1998) 555
- [10] P. Hoffmann-Rothe et al., Phys. Rev. Lett. **78** (1997) 4697
- [11] G. F. Chew, M. L. Goldberger, F. E. Low, Y. Nambu, Phys. Rev. **106** (1957) 1345
- [12] B. Borasoy, Phys. Rev. **D61** (2000) 014011;  
B. Borasoy, Eur. Phys. J. **A7** (2000) 255
- [13] Particle Data Group, C. Caso et al., Eur. Phys. J. **C3** (1998) 1
- [14] F. E. Close, R. G. Roberts, Phys. Lett. **B316** (1993) 165;  
B. Borasoy, Phys. Rev. **D59** (1999) 054021
- [15] O. Dumbrajs et al., Nucl. Phys. **B216** (1983) 277
- [16] S.-O. Bäckmann, G. E. Brown, J. A. Niskanen, Phys. Rep. **124** (1985) 1
- [17] B. Borasoy, U.-G. Meißner, Ann. Phys. **254** (1997) 192;  
B. Borasoy, Phys. Rev. **D59** (1999) 094025
- [18] B. Borasoy, Phys. Rev. **D59** (1999) 054019

## Table captions

Table 1 Given are the multipoles for  $\eta$  photoproduction off the proton at c.m. energy  $s = 708$  MeV both with and without resonances in units of  $10^{-3}/m_{\pi^+}$ . The first row denotes the contributions from only the Born terms. In the following rows we have added vector mesons, spin-1/2<sup>+</sup> and spin-1/2<sup>-</sup> baryon resonances, respectively. The last row gives our final result, including all resonances considered in this work.

## Figure captions

Fig.1 Shown are the Born terms for photoproduction on the proton. The photon is given by a wavy line. Solid and dashed lines denote proton and pseudoscalar mesons, respectively.

Fig.2 Vector meson exchange. The photon is given by a wavy line. Solid and dashed lines denote nucleons and pseudoscalar mesons, respectively. The double line represents the vector meson.

Fig.3 Baryon resonance contributions. The photon is given by a wavy line. Solid and dashed lines denote nucleons and pseudoscalar mesons, respectively. The double line represents the baryon resonances  $P_{11}(1440)$  or  $S_{11}(1535)$ .

Fig.4 Total cross sections for  $\gamma p \rightarrow p\eta$  (a),  $\gamma p \rightarrow p\eta'$  (b),  $\gamma n \rightarrow n\eta$  (c) and  $\gamma n \rightarrow n\eta'$  (d). The dashed lines denote the contributions from the Born terms, the full lines are our results including the resonances. The reaction  $\gamma p \rightarrow p\eta$  in (a) is compared with data from [1]. We do not show data from [9] for  $\eta'$  photoproduction since the energy bins of this experiment are 100 and 200 MeV wide.

Fig.5 a) Differential cross section of  $\gamma p \rightarrow p\eta$  for the photon energy  $E_\gamma = 716$  MeV which is compared with the data from [1].

b) Differential cross section for  $\gamma p \rightarrow p\eta'$  at  $E_\gamma = 1.45$  GeV. The data are the energy-integrated angular distributions for  $1.44 \text{ GeV} < E_\gamma < 1.54 \text{ GeV}$  [9].

Fig.6 Shown are the multipoles  $E_{0+}$  (a),  $M_{1+}$  (b),  $M_{1-}$  (c) and  $E_{1+}$  (d) for  $\eta$  photoproduction off the nucleons. The full and dashed lines denote  $\gamma p \rightarrow p\eta$  and  $\gamma n \rightarrow n\eta$ , respectively.

Fig.7 Shown are the multipoles  $E_{0+}$  (a),  $M_{1+}$  (b),  $M_{1-}$  (c) and  $E_{1+}$  (d) for  $\eta'$  photoproduction off the nucleons. The full and dashed lines denote  $\gamma p \rightarrow p\eta'$  and  $\gamma n \rightarrow n\eta'$ , respectively.

Fig.8 Energy dependence of the coefficients A (a), B (b), C (c) from Eq. (23) for  $\eta$  photoproduction. The full and dashed lines denote  $\gamma p \rightarrow p\eta$  and  $\gamma n \rightarrow n\eta$ , respectively.

Fig.9 Energy dependence of the coefficients A (a), B (b), C (c) from Eq. (23) for  $\eta'$  photoproduction. The full and dashed lines denote  $\gamma p \rightarrow p\eta'$  and  $\gamma n \rightarrow n\eta'$ , respectively.

	$E_{0+}$	$M_{1+}$	$M_{1-}$	$E_{1+}$
$N$	-4.47	0.073	-0.10	0.009
$N, V$	2.48	0.084	0.27	-0.006
$N, P_{11}$	-4.40	0.079	-0.32	0.009
$N, S_{11}$	6.36	0.076	-0.09	0.008
$N, V, P_{11}, S_{11}$	13.39	0.092	0.06	-0.007

Table 1

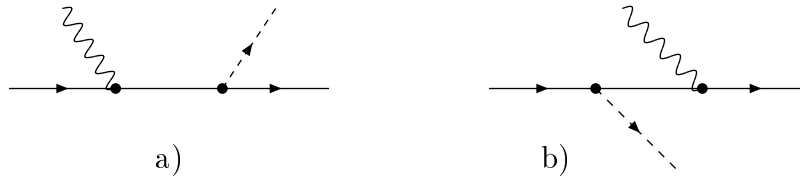


Figure 1

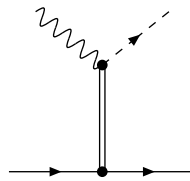


Figure 2



Figure 3

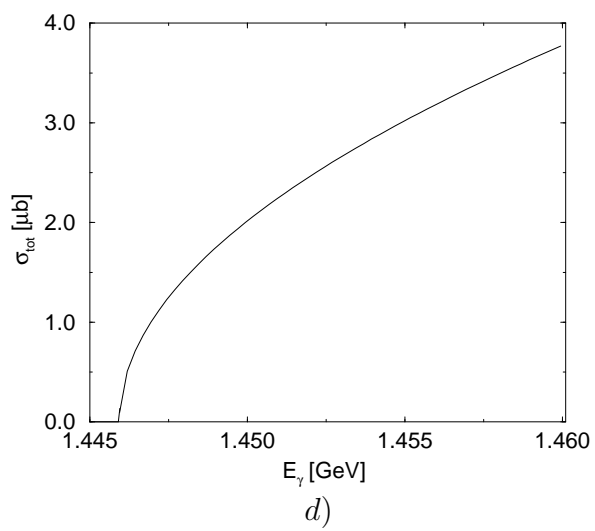
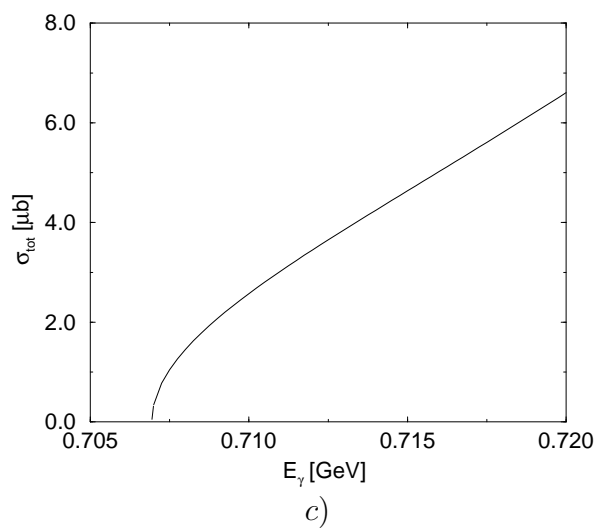
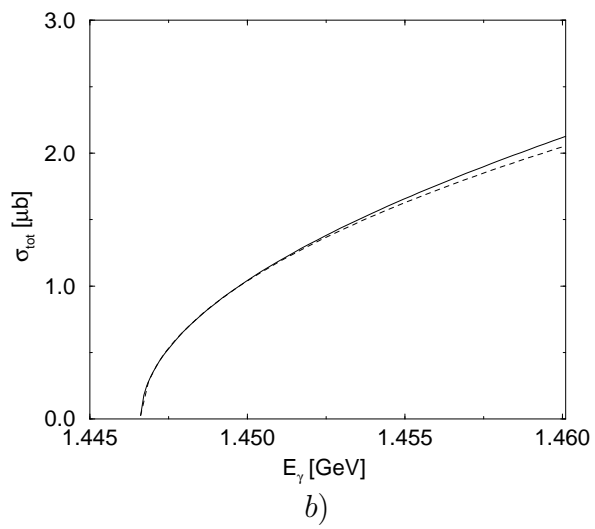
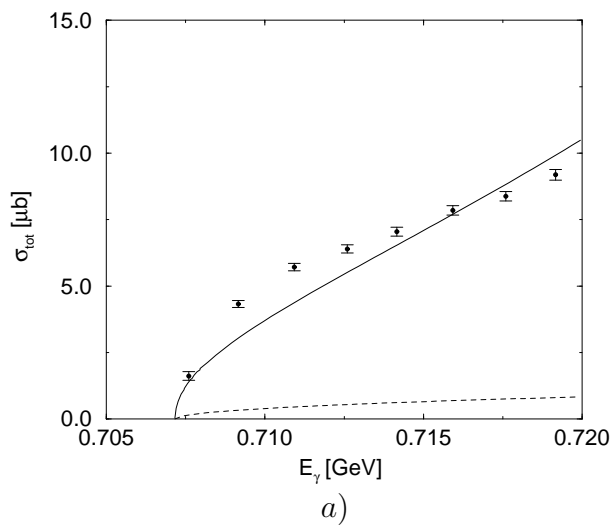
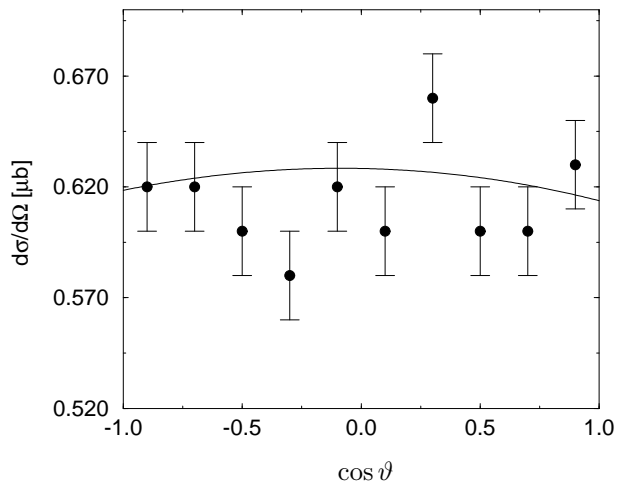
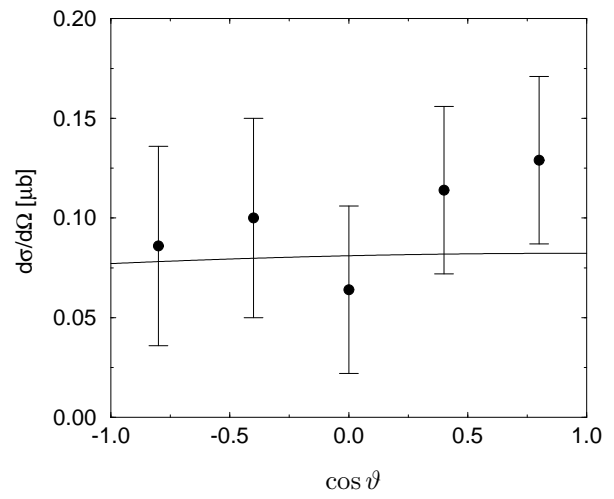


Figure 4



a)



b)

Figure 5

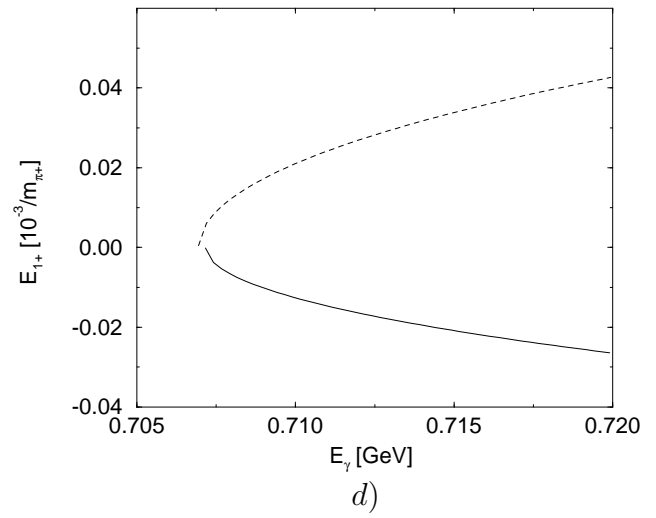
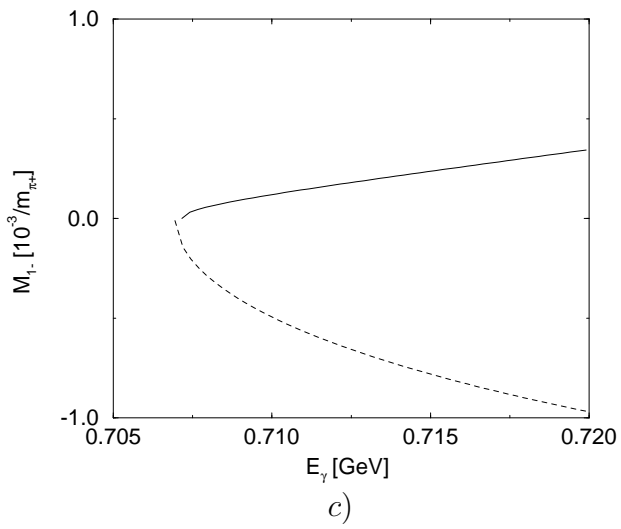
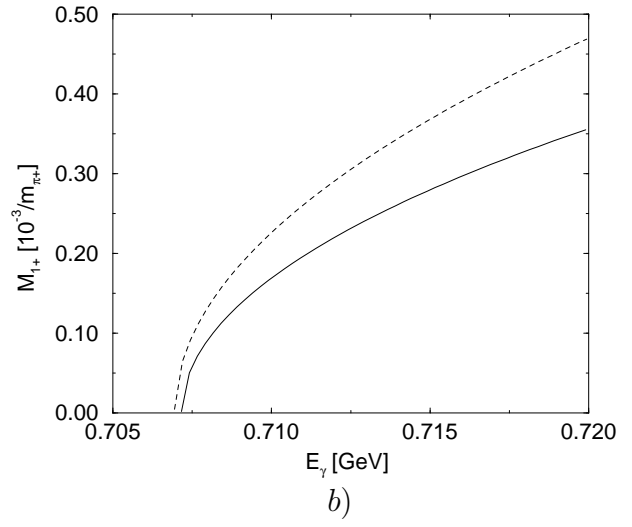
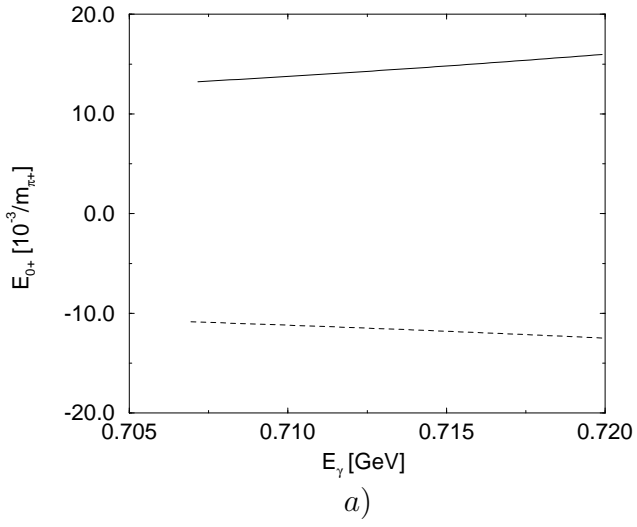


Figure 6

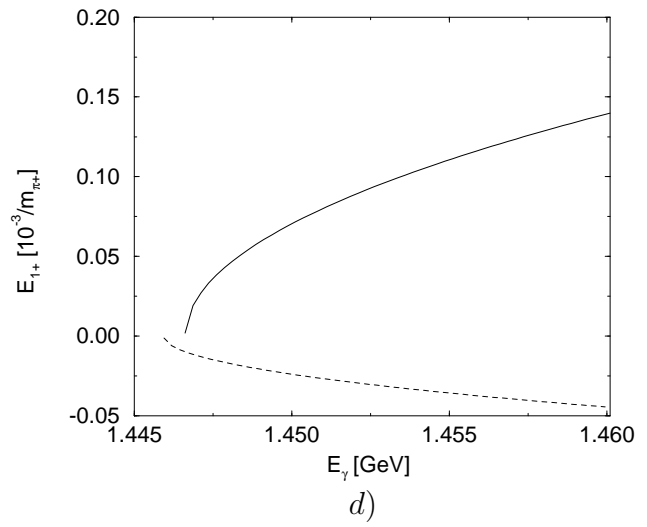
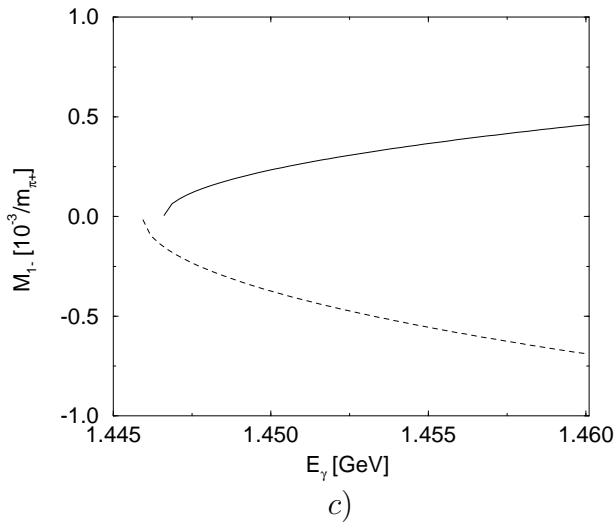
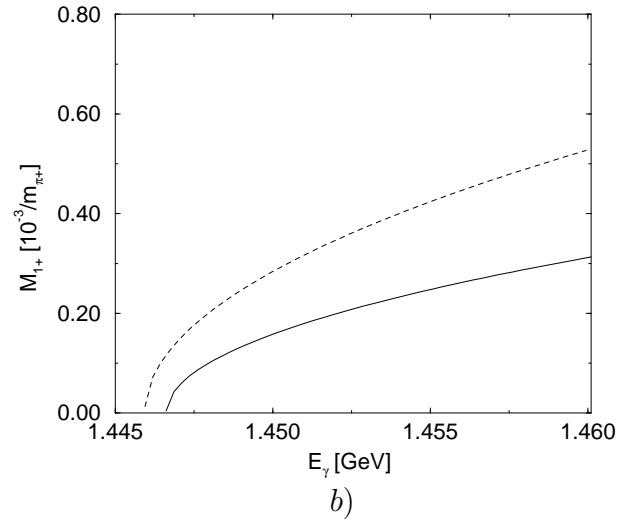
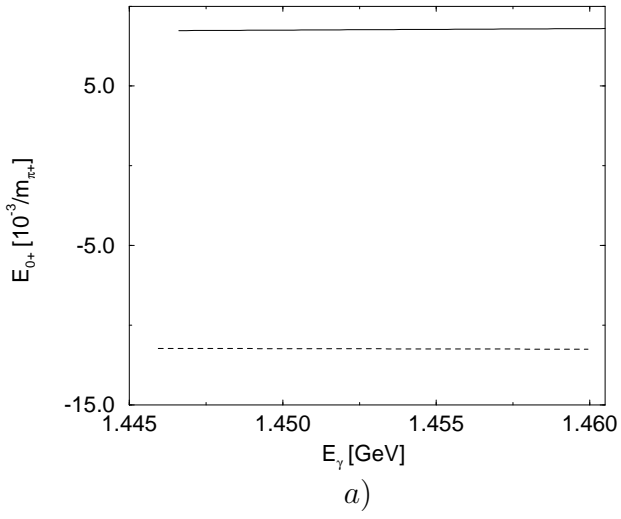


Figure 7

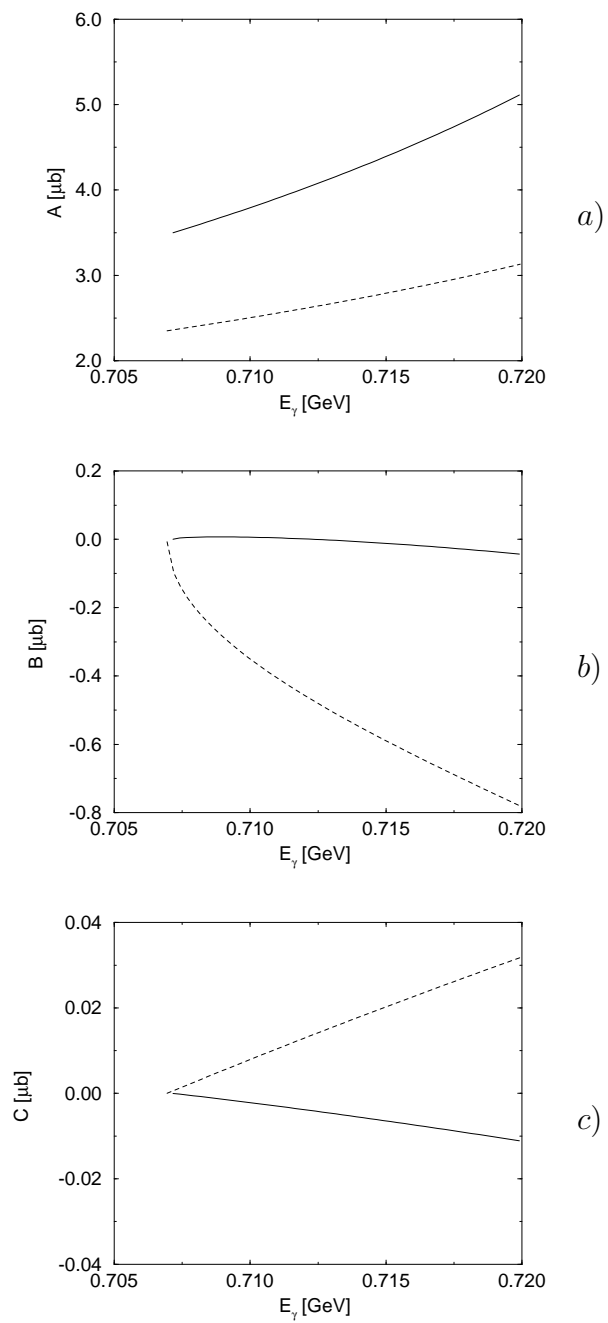


Figure 8

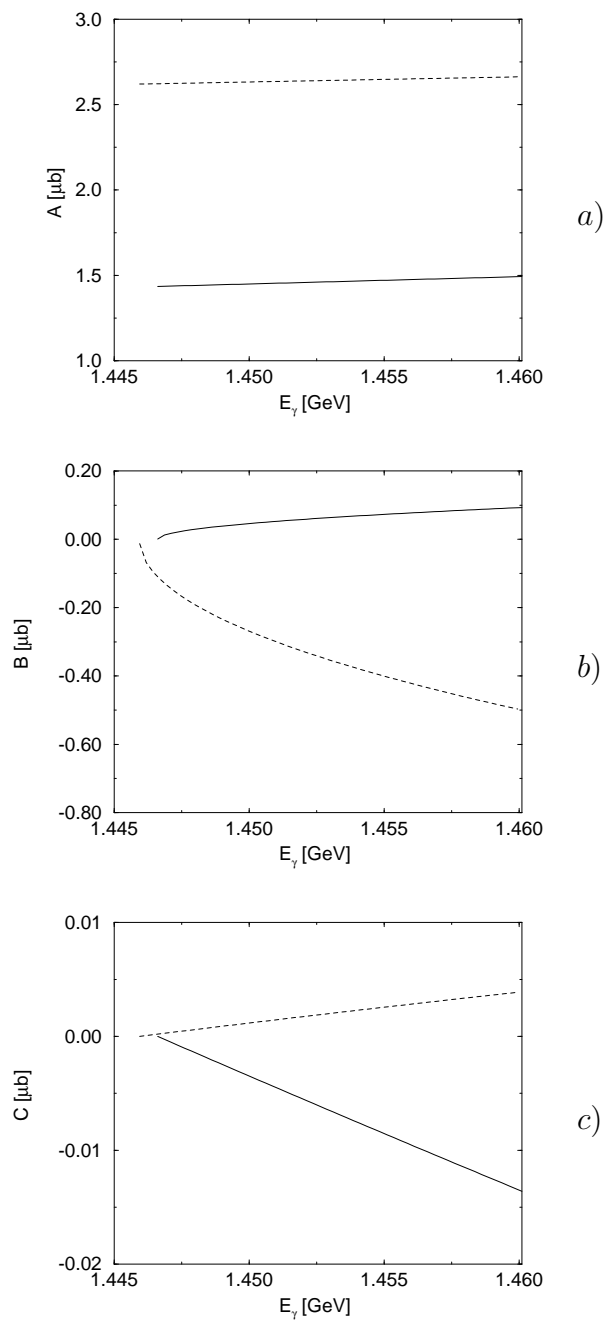


Figure 9